

Utilisation of transition metal chalcogenide MoSe₂ as promising antireflective coating for achieving intensified light trapping

S. Santhosh^a, R. Rajasekar^{a,*}, V. K. Gobinath^b, C. Moganapriya^a, A. Manju Sri^c

^a*Department of Mechanical Engineering, Kongu Engineering College, Perundurai, Erode-63806, India*

^b*Department of Mechatronics Engineering, Kongu Engineering College, Perundurai, Erode-638060, India*

^c*Department of Chemical Engineering, Kongu Engineering College, Perundurai, Erode-638060, India*

At present scenario, engineering renewable energy sources with the view of attaining maximum efficiency is more important. The current research focusses on the synthesis and deposition of molybdenum diselenide over solar cell surface for achieving maximum light transmissivity. MoSe₂ nanostructures synthesised through hydrothermal method exhibit excellent antireflection property. The developed transition metal chalcogenide is pelletised and sputter coated over solar cell substrate at regular intervals. Coated samples were analysed through various characterisation techniques from which S3 sample exhibited minimum light transmittance and electrical resistivity. The MoSe₂ coating with 648 nm thickness reported maximum power conversion efficiency of 19.45 %.

(Received March 29, 2021; Accepted June 17, 2021)

Keywords: Silicon solar cell, Molybdenum diselenide, Power conversion efficiency, Transmittance

1. Introduction

Conventional Si solar cells are one of the most successful solar cells in the photovoltaic market. Crystalline Si solar cells possess better stability and longer working span. Crystalline Si were categorized into mono-crystalline Si and Polycrystalline Si[1]. The fabrication cost of mono-crystalline Si is high, as they were fabricated from single source of Si, while Polycrystalline Si were synthesised from blending various sources of Si. Hence Polycrystalline Si solar cell were mostly preferred due to their lower fabrication cost. In spite of these properties, some of the losses were encountered in solar cell which hinders the cell performance. Some of the major losses in solar cell are electrical and reflection loss. The reflection loss can be controlled by surface texturing and antireflection coatings (ARC) over the surface of solar cell. Surface of solar cell was etched with the help of etchants leads to the formation of nanostructures over the surface resulting in enhanced trapping of incident light[2]. Antireflective coating materials are optical coating generally used to reduce reflection of incident light. In other words, ARC improves absorption and transmission of light. Some of the antireflection materials are TiO₂, MgF₂, Al₂S₃, ZnAl₂O₄, SiO₂, SnO₂, MoS₂ etc., ARC materials can be coated through Physical and chemical vapour deposition technique[3]. Light can be trapped effectively through two ways: maintaining constant antireflective coating material with increase in coating thickness and different material coatings over the solar cell surface[4].

Strong thin film coatings can be achieved through PVD technique. Anti-reflective property materials with electrical conductivity might improve the charge carrier transportation and optical transmissivity. Transition metal chalcogenides also capable of converting incident photons into equivalent electrical energy[5]. MoSe₂ holds better anti-reflective property, minimum electrical resistance and low fabrication cost. In addition to this, aluminium based transition metal chalcogenide MoSe₂ films have wider band gap of about 1.8 eV.¹

*Corresponding author: rajasekar.cr@gmail.com
<https://doi.org/10.15251/CL.2021.186.327>

The thin film anti-reflection coatings were deposited using several deposition techniques such as dip coating, sol-gel process, blade coating, spin coating, sputter coating, plasma enhanced CVD, electro-spraying and thermal oxide growth. Among them, sputter deposition technique paves the way for the uniform deposition of material over the target surface[6]. Power based materials can be converted into pellets and then employed in the sputter deposition process. Meanwhile, solution dispersed particles at optimal rotational disc speed and flow rate, uniform thickness can be achieved through spin coating technique[7]. However, improper AR coating over substrate may lead to certain drawbacks such as poor adherence, lower working life and higher operating cost. Hence machining parameters should be optimised for obtaining effective AR coating over the surface of solar cell[8]. Some of the notable input parameters in RF sputter coating technique are distance between substrate and target, temperature of the substrate, incoming gas pressure, deposition time, input power, target material, deposition type (RF or DC sputtering) and type of inlet gas used. However, for validation purpose certain parameters should be maintained constant while others varied in regular intervals[9]. Set of experiments were been conducted through sputter technique for thin film AR coating over solar cell surface. Effective AR coating with appropriate coating materials might reduce the reflectivity through subsequent improvement in transmissivity and absorptivity[10]. The bare cell efficiency was found initially as 13.61 %.

In this experimental work, MoSe₂ metal chalcogenide with wide energy band gap holds better antireflective property for attaining higher transmissivity. The hydrothermally synthesised MoSe₂ was deposited over polycrystalline Si solar cell through RF sputtering technique. The optimal operating machining parameters is found to be 150W sputter power, 5cm target-substrate distance and Ar atmosphere. The electrical, optical, structural, morphological studies of 2D-transition metal chalcogenide coated material were evaluated through various characterisation techniques such as Fe-SEM with EDAX, XRD, AFM, TEM, UV-Visible spectroscopy, I-V measurement, Four Probe method and thermal imaging[11].

2. Materials and methods

Polycrystalline silicon solar cell was purchased from Solar India with an average output efficiency of 13.61 %.

2.1. Synthesis of MoSe₂

Molybdenum Diselenide can be synthesised easily through hydrothermal method. Initially, the precursor chemicals such as Sodium molybdate dihydrate, Sodium borohydride and Se powder were purchased from Sigma Aldrich. Initially, 1.7 g of Sodium molybdate dihydrate and 1.6 g of selenide powders were mixed together for about 2 minutes. Then the mixture is magnetically stirred at 1400 rpm in 0.05L of distilled water and ethyl alcohol for about 30 minutes. Further the completely dissolved mixture was transferred to 100 ml autoclave. Quick after the transfer of solution, required quantity of H₂N₂O solution was added with the stirred mixture. Consequently, the mixture is subjected to high-speed stirring for 25 minutes. The ph value of the mixture was then calculated, and a sufficient amount of sodium hydroxide solution was applied until the ph value of the mixture reaches 12. Following that, 75% of the autoclave is filled with distilled water. The autoclave is now sealed, and the temperature is set for 48 hours at 190°C. Further, the autoclave was cooled at room temperature resulting in the formation of black coloured precipitate. It is then collected and washed continuously with ethyl alcohol and distilled water. After that, it was dried for 9 hours at 60°C in a hot air oven, which resulted in the formation of MoSe₂. The synthesised transition metal chalcogenide was utilised for the target preparation

2.2. Sputter deposition of MoSe₂

Initially, the procured solar cells were cleaned using acetone and isopropyl alcohol with the help of ultra-sonicator. Then solar cell is dried and then mounted over the holder for surface coating. For the sputter deposition process, the target material which is to be coated over the solar cell surface must be in the form of solid pellet. The approximate dimension of pellet is found to be

5 cm diameter and 5 mm thickness. The average quantity of synthesised powder required for the pelletisation process is 15 g. The synthesised 2D- transition metal chalcogenide was filled into the mild steel die. The die surfaces were pre-cleaned using ethanol followed by coating nickel over the bottom plate for facilitating easier removal of pellet [12]. The MoSe₂ filled die is then subjected to compressive stress of 1.3 GPa lead to the formation of appropriate target material for sputter deposition technique. The sputter deposition equipment for coating antireflection materials is depicted in Fig. 1.



Fig. 1. Sputter deposition equipment for antireflection coating over Poly-Si solar cell.

With the high voltage supply, plasma gets generated between the target and substrate under inert atmosphere as indicated in Fig. 2. The argon gas gets bombarded with the target material and sputters off. Due to high vacuum and plasma generation, the ions expelled from the target then deposit over the solar cell surface[2]. The effect of plasma generation, sputter power, sputtering time, inert atmosphere and target-substrate distance influences the quality of sputter deposition as represented in Table 1. For instance, increasing sputter power increases the rate of sputtering process. Sputter power makes the argon gas bombard with the target material. Initially minimum amount of material gets bombarded and expels out the material[4]. Excessive power makes the deposition at higher rate which leads to the increase in surface roughness, internal cracks, internal stress and crystal defects. Hence, sputter power of 150 W is considered to be optimal power for sputter deposition of transition metal chalcogenide (MoSe₂). Sputter power have influence over the surface morphology. Particle size and roughness increases with increase in sputter power[6].

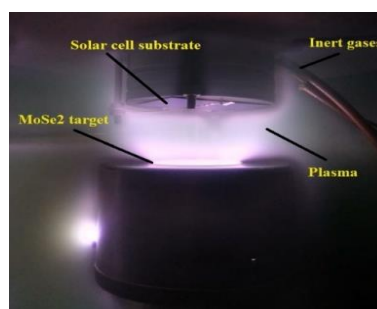


Fig. 2. MoSe₂ deposition on solar cell target.

Table. 1 Sputter deposition operating parameters.

S.No	Operating Machining Parameters	Specification
1	Sputter power	150 W
2	Distance between target and substrate	4 cm
3	Operating atmosphere	Ar
4	Sputtering time	15,30,45 and 60 minutes
5	Operating temperature	Ambient temperature
6	Working pressure	6 Pa

2.3 Evaluation of properties of MoSe₂ Chalcogenide coating

The crystallographic structure and nature of crystallinity were investigated through X-ray diffraction technique. Hydrothermally synthesised target material is found to be in hexagonal crystal structure[13].

The thickness and cross-sectional view of various thin film coatings were determined through FESEM analysis[14]. The coated particles over solar cell substrate are deposited uniform and found to be dense in nature. As sputter deposition time increases, the grain size of the coating material increases. The chemical composition of various elements of thin film coatings. The peaks of EDS indicate the existence of various elements through x-ray interaction with the sample[15]. The major peak will denote the major constitution of sample, while the minor peaks represent the presence of Al, Zn and S as supplementary elements. The surface morphology and surface roughness can be viewed clearly in 2 dimensional and 3 dimensional aspects. The incident light transmittance and absorbance of various coated samples can be studied through UV-Vis spectroscopy. This study reveals the optimal antireflective coating led to maximum solar cell efficiency[16]. The electrical resistivity of coated solar cell samples can be evaluated through four-point probe method. I-V characteristic study of coated samples were performed by Keithley I-V source meter. Finally, the effect of temperature on coated solar cell samples can be analysed through Fluke thermal imaging camera[17].

3. Result and discussion

The thickness of coated samples as explored from AFM analysis are 394 nm, 489 nm, 628 nm and 910 nm as represented in Fig. 3. In addition to this, the Root Mean Square values of coated surface roughness for S1, S2, S3 and S4 are 32 nm, 37 nm, 45 nm and 52 nm. From experimental results, it is observed that thickness of coating, grain size and surface roughness increase with subsequent increase in sputter deposition time[18].

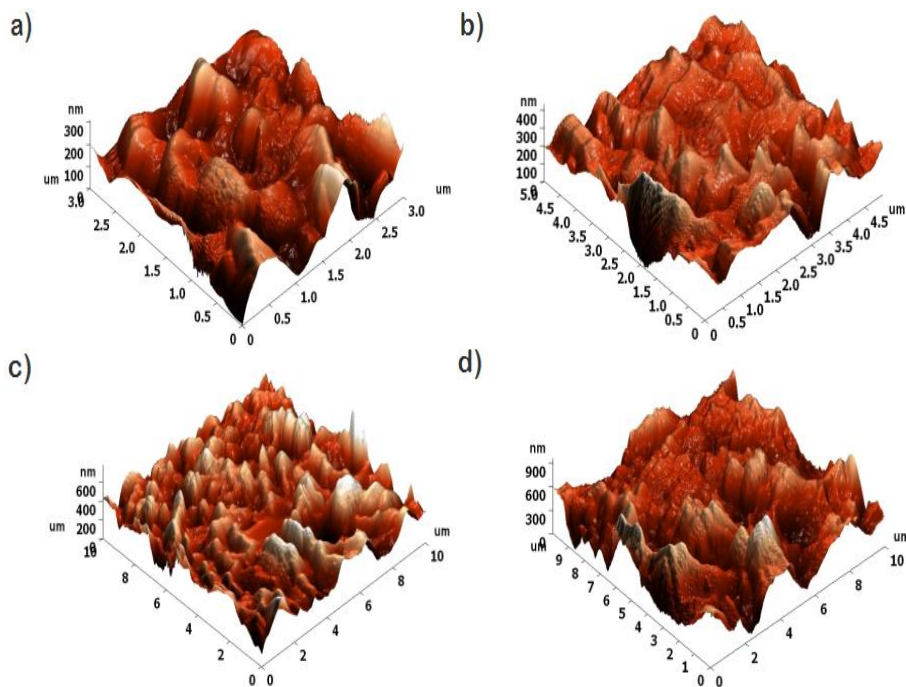


Fig. 3. AFM images depicting surface morphology and surface roughness of coated samples a) S1, b) S2, c) S3 and d) S4.

In general, single material coating have capability of absorbing the incident photons that too in specific energy range. Other than the specified energy range, the remaining photons were simply absorbed by the solar cell and do not involve in the photo-conversion process[14]. The multilayer coating is much similar with the tandem architecture, as high energy photons in addition to low energy photons shall be utilised for the effective power conversion process. In Multilayer AR coating, the utilisation of incident light at various coated layers seemed to be in increasing order while leaving minimum quantity of reflected and absorbed photons[19]. It is noted that agglomeration of smaller crystals occurs at some areas which further lead to the decrease in light transmittance. The FESEM images of bare and S3 coated sample were indicated in Fig. 4 (a) & (b).

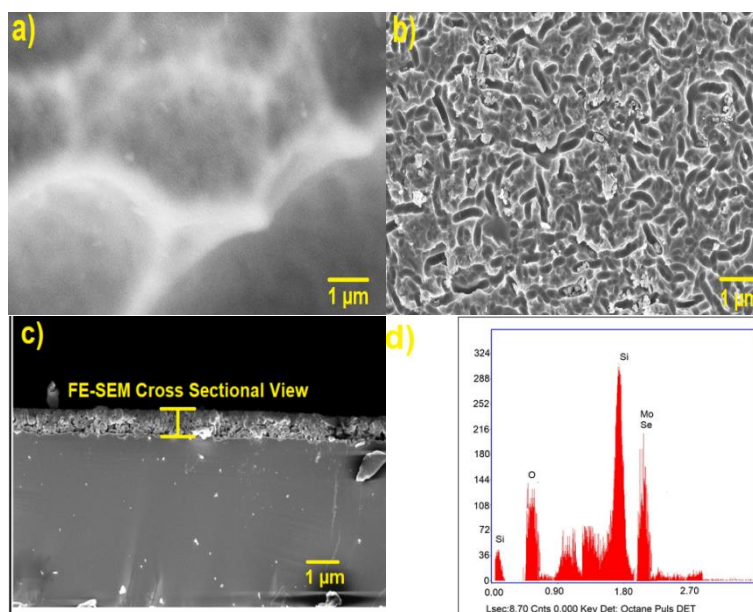


Fig. 4. FESEM images a) uncoated solar cell b) S3 coated sample c) cross-sectional image of coatings d) EDAX analysis of S3 sample.

The cross-sectional view of the optimal coated solar cell with maximum efficiency of 19.45% and 19.08 % under closed and open operating condition was clearly represented in figure 4 (c). The coated material over the polycrystalline Si solar cell was confirmed through EDAX analysis. Figure. 4 (d) represents the existence of various elements in the optimal surface coating of MoSe₂. Various concentrations of elements present in the coated solar cell can be determined through EDAX analysis[20]. The maximum peak obtained for Si is mainly due to the existence of polycrystalline Silicon as photoactive material in solar cell.

The electrical resistivity of various sputter coated films was measured with the help of four probe technique were tabulated in Table. 2. Up to 45 minutes of sputter deposition time the electrical resistivity found to be decreasing[21]. This is especially due to the presence of Mo element in the coating. Beyond 45 minutes of sputter deposition, there occurs larger crystal growth and grain size with no deviation in crystal orientation.

Table. 2 Electrical resistivity of different coated solar cell samples.

S.No	Solar cell samples	Electrical Resistivity (Ω -cm)
1	Uncoated solar cell	6.77×10^{-3}
2	S1	5.63×10^{-3}
3	S2	3.70×10^{-3}
4	S3	2.83×10^{-3}
5	S4	3.19×10^{-3}

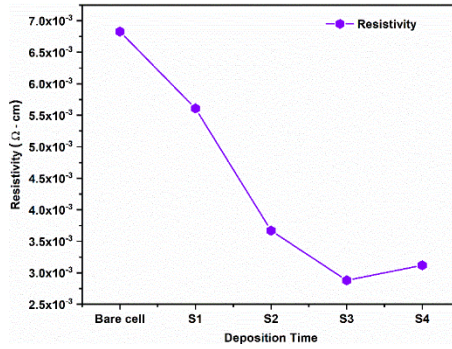


Fig. 5. Electrical resistivity of coated samples in accordance with different coating times.

This offers resistance to light transmission which leads to drop in solar cell performance. The minimum electrical resistivity achieved at 628 nm thickness is found to be $2.83 \times 10^{-3} \Omega\text{-cm}$ and graphically represented in Fig. 5. Electrical conductivity increases with subsequent decrease in electrical resistivity[21]. The carrier concentration and hall mobility increases upto the coating thickness of 628 nm. Further increase in coating thickness ends up with decline in hall mobility and carrier concentration[22]. Hence, layer with minimum electrical resistivity exhibits maximum solar cell performance of **19.45%**.

The energy band gap of the various coated solar cells were found to be 1.97 eV, 1.89 eV, 1.80 eV and 1.73 eV. The band gap of various sputter deposited coatings can be calculated through the incorporation of some modifications in Kubelka-Munk remission function[23]. The energy dependent absorbance coefficient (α) can be related with the reflectance at infinite surface, hence the energy band gap of metal chalcogenide coating can be evaluated through the following equation (1).

$$(\alpha \times h \times \nu)^{\frac{1}{2}} = D(h \nu - E_g) \quad (1)$$

where h is Planck’s constant, ν is frequency of electromagnetic radiation, E_g is referred as energy band gap and D is a constant. It is found that bandgap decreases with the increase in coating thickness due to localisation of valence band fitted with higher number of electrons. The optimal antireflection coating has 1.8 eV of energy band gap clearly indicated in Fig. 6.

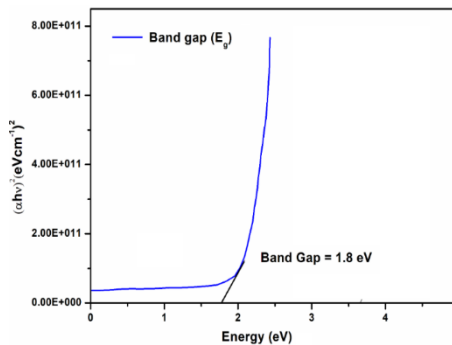


Fig. 6. Energy bandgap of optimal coated solar cell (S3).

The main aim of coating antireflective materials over the solar cell surface is reduce the proportion of reflectance with the subsequent improvement in transmittance and absorbance. The relation between the transmissivity (τ), absorptivity (α) and reflectivity (ρ) is represented in the relation (2).

$$\tau + \alpha + \rho = 1 \quad (2)$$

The influence of antireflection coating with respect to the optical transmittance can be studied using UV-Vis spectroscopy[24]. The coated solar cell samples exhibit better optical transmittance in the visible range of wavelength 350 to 800 nm. From experimental results, it is evident that light transmittance increases upto 45 minutes of coating sample. This is due to the minimal scattering of incident photons at the coating surface. Beyond that there is decrease of optical transmissivity due to increased absorptivity and reflectivity which is graphically indicated in Fig. 7 and tabulated in Table 3.

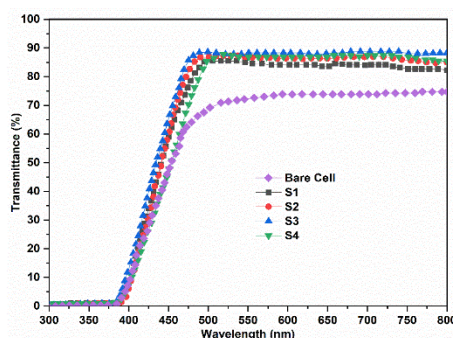


Fig. 7. Transmittance of various MoSe_2 coated samples.

Hence optimisation of coating thickness with reference to sputtering time is quite important for attaining maximum solar cell performance. Aggregation of coating material over the cell surface because of longer sputtering time, S4 sample experiences huge amount of photon scattering. This is the reason for declined solar cell performance for sample S4.

Table. 3 optical reflectance and transmittance of various solar cell samples.

S.No	Solar Cell samples	Sputtering time (min)	Optical transmittance (%)	Optical reflectance (%)	Coating thickness (nm)
1	Uncoated solar cell	0	70.2	25	0
2	S1	15	85.6	13.2	394
3	S2	30	87	10.9	489
4	S3	45	89.3	7.5	628
5	S4	60	85.1	12	910

In closed source, the artificial solar radiation flux seemed to be constant. The controlled operating atmosphere for photo-energy generation was achieved through tailor made solar simulator. The solar simulator comprises of neodymium bulb with an output of 1 sun radiation, solar cell mounting, solar power meter and thermal imager. Initially the coated samples were placed in the solar cell mounting, the solar cell is connected with the I-V source meter. Now the neodymium light is switched on. The output of solar cell was monitored through I-V source meter. Power conversion efficiency shows the performance of solar cell and can be calculated mathematically using relation (3). The power conversion efficiency is the ratio of output energy from solar cell to incident photon energy.

$$\eta = \frac{I_{sc} \times V_{oc} \times FF}{P_{in}} \quad (3)$$

Due to very minimal fluctuation in solar radiation, the overall efficiency likely higher than the open atmospheric condition. The maximum solar cell efficiency of 19.45% was achieved for S3 coated sample under closed condition. The plot between the current density and voltage drawn at the time of photo-conversion process of various coated samples is graphically mentioned in Fig. 8.

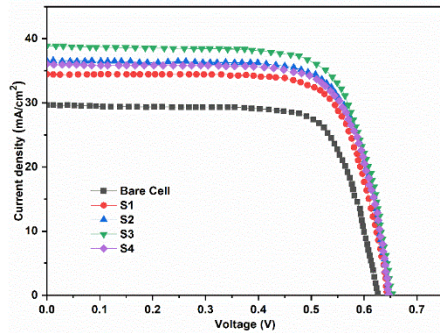


Fig. 8. J-V characteristic curve of various coated and uncoated solar cells Under closed-source condition.

It is found that fill factor increases with increase in efficiency and vice versa. For sample of 45 minutes of coating with coating thickness and surface roughness as 628 nm and 45 nm shows maximum solar cell efficiency. The current density and Voc for various samples were represented in the following Table 4.

Table. 4 power conversion efficiency of various coated and uncoated solar cells under closed-source condition.

S.No	Solar cell samples	Coating time (min)	Jsc (mA/cm ²)	Voc (V)	FF	η (%)
1.	Uncoated solar cell	0	29.96	0.631	0.72	13.61
2.	S1	15	34.49	0.639	0.74	16.31
3.	S2	30	36.68	0.641	0.77	18.10
4.	S3	45	38.8	0.643	0.81	19.45
5.	S4	60	35.87	0.632	0.79	17.91

The coated solar cell samples interconnected with Keithley I-V source meter were placed in the direct sunlight[25]. The solar power meter and thermal imager are utilised for measuring solar radiation flux and temperature of solar cell. Kick-start software is used for interfacing the I-V source meter with the display unit. In open source, the solar radiation flux continuously varies from time to time. Hence, solar cell under open-source condition experiences slightly lesser efficiency as compared to closed atmospheric condition. I-V characteristic curve is predominantly required for the calculation of power conversion efficiency which is tabulated in Table 5.

Table 5. Power conversion efficiency of various coated and uncoated solar cells under open-source condition.

S.No	Solar cell samples	Coating time (min)	Jsc (mA/cm ²)	Voc (V)	FF	η (%)
1.	Uncoated solar cell	0	28.30	0.627	0.72	13.45
2.	S1	15	32.69	0.635	0.74	15.84
3.	S2	30	35.06	0.638	0.76	18.68
4.	S3	45	36.97	0.640	0.75	19.08
5.	S4	60	33.92	0.629	0.79	18.32

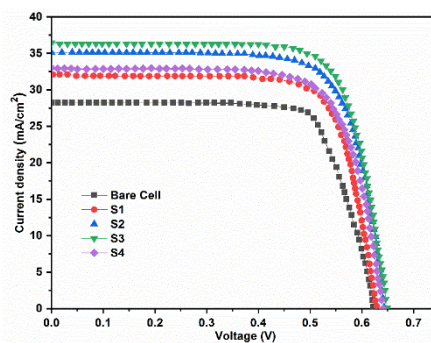


Fig. 9. J-V characteristic curve of various coated and uncoated solar cells under open-source condition.

The solar cell efficiency is also depending on shunt and series resistance offered by the solar cell at the time of photo-energy generation. The plot between current density (mA/cm²) and voltage (V) reveals the behaviour of voltage and current for various MoSe₂ coated samples. Among them, S3 solar cell sample exhibits maximum efficiency of 19.08 %. The pictorial representation of J-V characteristic curve of various coated and uncoated solar cells under open-source condition is shown in Fig. 9

During energy conversion process, the temperature of coated solar cell samples was measured. Infrared thermal imaging device is used to measure the surface temperature of solar cell under light irradiation[26]. In open source, the temperature of solar cell samples S1, S2, S3 and S4 found to be 45.1° C, 42.4° C, 39.7° C and 43.2° C respectively. Meanwhile, samples S1, S2, S3 and S4 cell temperature under closed source found to be 56.7° C, 53.2° C, 51.4° C and 54° C. In both open and closed conditions, sample with optimal coating thickness 628 nm experiences maximum solar cell efficiency as in Fig. 10.

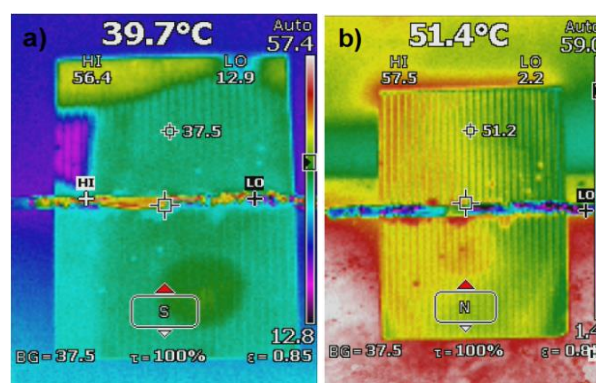


Fig. 10. Thermal image of optimal solar cell (S3) under open and closed conditions.

4. Conclusions

Transition metal chalcogenide MoSe₂ was synthesised using facile hydrothermal method. Then synthesised metal chalcogenide is deposited over different solar cells at frequent time intervals under argon atmosphere. Based on the resistivity analysis, it is clearly depicted that 45 minutes coated sample experiences maximum hall mobility and carrier concentration. Through AFM analysis, the coating thickness and roughness are found to be in the range of 394 to 910 nm and 32 to 52 nm. Maximum transmittance of 89.3 % and 19.45 % efficiency achieved at 45 minutes coated sample proves maximum utilisation of incident photons.

The minimum electrical resistivity for optimal solar cell (S3) is found to be $2.83 \times 10^{-3} \Omega\text{-cm}$. From J-V studies, S3 sample reported maximum I_{sc} and V_{oc} which indirectly responsible for the increase in efficiency from 13.61 to 19.45%. Then continual increasing the coating thickness led to decrement in solar cell performance. It is also evident that solar cell performance decreases with increase in cell temperature under illumination. Hence MoSe₂ was found to promising antireflective coating for increasing the power conversion efficiency of solar cell.

Acknowledgements

S. Santhosh thanking AICTE, New Delhi for selecting as full-time research scholar under National Doctoral Fellowship (NDF) scheme in 2019 (Scholar ID-1-6382526181).

References

- [1] G.V. Kaliyannan, S.V. Palanisamy, M. Palanisamy, M. Subramanian, P. Paramasivam, R. Rathanasamy, *Materials Science Poland* **37**, 2019.
- [2] G.V. Kaliyannan, S.V. Palanisamy, R. Rathanasamy, M. Palanisamy, N. Nagarajan, S. Sivaraj, M.S. Anbupalani, *Journal of Electronic Materials* **49**(10), 2020.
- [3] G.V. Kaliyannan, S.V. Palanisamy, M. Palanisamy, M. Chinnasamy, S. Somasundaram, N. Nagarajan, R. Rathanasamy, *Applied Nanoscience* **9**(7), 2019.
- [4] G.V. Kaliyannan, S.V. Palanisamy, R. Rathanasamy, M. Palanisamy, S.K. Palaniappan, M. Chinnasamy, *Journal of Materials Science: Materials in Electronics* **31**(3), 2020.
- [5] R. Manivannan, S.N. Victoria, *Solar Energy* **173**, 2018.
- [6] P. Gu, X. Zhu, J. Li, H. Wu, and D. Yang, *Journal of Materials Science: Materials in Electronics* **29**(17), 2018.
- [7] G.V. Kaliyannan, S.V. Palanisamy, E. Priyanka, S. Thangavel, S. Sivaraj, R. Rathanasamy, *Materials Today: Proceedings*, 2020.
- [8] U. Sikder, M.A. Zaman, *Optics & Laser Technology* **79**, 2016.
- [9] C.-F. Fu, L.-F. Han, and C. Liu, *Journal of Materials Science: Materials in Electronics* **26**(1), 2015.
- [10] M. Chen, Z. Pei, X. Wang, C. Sun, L. Wen, *Journal of Vacuum Science & Technology A: Vacuum, Surfaces, and Films* **19**(3), 2001.
- [11] H. Tang, K. Dou, C.-C. Kaun, Q. Kuang, S. Yang, *Journal of materials chemistry a* **2**(2), 2014.
- [12] N. Ghobadi, M. Shiravand, and E.G. Hatam, *Optical and Quantum Electronics* **53**(1), 2021.
- [13] S.-Y. Yeo, T.-H. Kwon, C.-S. Park, C.-I. Kim, J.-S. Yun, Y.-H. Jeong, Y.-W. Hong, J.-H. Cho, J.-H. Paik, *Journal of Electroceramics* **41**(1-4), 2018.
- [14] P. Prepelita, M. Filipescu, I. Stavarache, F. Garoi, D. Craciun, *Applied Surface Science* **424**, 2017.
- [15] U. Gangopadhyay, K. Kim, D. Mangalaraj, J. Yi, *Applied Surface Science* **230**(1-4), 2004.
- [16] R. Sharma, G. Amit, V. Ajit, 2017.
- [17] E. Radziemska, *Progress in Energy and Combustion Science* **29**(5), 2003.
- [18] W. Vallejo, E. Romero, G. Gordillo, *Journal of the Brazilian Chemical Society* **22**(12), 2011.
- [19] S. Ghosh, S. Das, A. Sil, P.K. Biswas, *Journal of sol-gel science and technology* **64**(3), 2012.

- [20] W. Tian, B. Xi, Z. Feng, H. Li, J. Feng, S. Xiong, *Advanced Energy Materials* **9**(36), 2019.
- [21] Z. Xiong, W. Hu, Y. She, Q. Lin, L. Hu, X. Tang, K. Sun, *ACS applied materials & interfaces* **11**(33), 2019.
- [22] M. Ojha, M. Deepa, *Chemical Engineering Journal* **368**, 2019.
- [23] P. Makuła, M. Pacia, W. Macyk, *How to correctly determine the band gap energy of modified semiconductor photocatalysts based on UV–Vis spectra*, 2018, ACS Publications.
- [24] J. Pan, M.I.B. Utama, Q. Zhang, X. Liu, B. Peng, L.M. Wong, T.C. Sum, S. Wang, Q. Xiong, *Advanced Materials* **24**(30), 2012.
- [25] I.B. Karki, *Journal of Nepal Physical Society* **3**(1), 2015.
- [26] F. Liu, J. Zhu, L. Hu, B. Zhang, J. Yao, M.K. Nazeeruddin, M. Grätzel, S. Dai, *Journal of Materials Chemistry A* **3**(12), 2015.